

High resolution simulations of supersonic turbulence in molecular clouds

Alexei G. Kritsuk, Rick Wagner, Michael L. Norman, and Paolo Padoan
*Department of Physics and Center for Astrophysics and Space Sciences,
University of California, San Diego, 9500 Gilman Drive, La Jolla, CA
92093-0424*

Abstract. We present the results of three-dimensional simulations of supersonic Euler turbulence with grid resolutions up to 1024^3 points. Our numerical experiments describe nonmagnetized driven turbulent flows with an isothermal equation of state and an rms Mach number of 6. We demonstrate that the inertial range scaling properties of turbulence in this strongly compressible regime deviate substantially from a Kolmogorov-like behavior previously recovered for mildly compressible transonic flows.

1. Introduction

Understanding the nature of supersonic turbulence is of fundamental importance in astrophysics and in aeronautical engineering. In the interstellar medium, highly compressible turbulence is believed to control star formation in dense molecular clouds. A whole class of more *terrestrial* applications deals with the drag and stability of projectiles traveling through the air at hypersonic speeds.

Molecular clouds have a highly inhomogeneous structure and the intensity of their internal motions corresponds to an rms Mach number of the order of 20. Larson (1981) has demonstrated that within the range of scales from 0.1 pc to 100 pc, the gas density and the velocity dispersion tightly correlate with the cloud size.¹ Supported by other independent observational facts indicating scale invariance, these relationships are often interpreted in terms of supersonic turbulence with characteristic Reynolds numbers $Re \sim 10^8$. Within a wide range of densities around 10^3 cm^{-3} the gas temperature remains close to ≈ 10 K since the thermal equilibration time at these densities is shorter than a typical hydrodynamic time scale. Thus, an isothermal equation of state can be used as a reasonable approximation. While self-gravity, magnetic fields, chemistry, cooling and heating, as well as radiative transfer should be ultimately accounted for in turbulent models of molecular clouds, we focus here specifically on hydrodynamic aspects of the problem.

Numerical simulations of *decaying* supersonic hydrodynamic turbulence with the piecewise parabolic method (Colella & Woodward 1984, PPM) in two dimensions were pioneered by Passot et al. (1988)² and then followed up with

¹See Kaplan & Pronik (1953) for an earlier version of what is now known as Larson’s relations.

²See a review on compressible turbulence by Pouquet et al. (1991) for references to earlier works.

high resolution 2D and 3D simulations by Porter et al. (1992a,b, 1994, 1998). Sytine et al. (2000) compared the results of PPM Euler computations with PPM Navier-Stokes results and showed that Euler simulations agree well with the high- Re limit attained in the Navier-Stokes models. The convergence in a statistical sense as well as the direct comparison of structures in configuration space indicate the ability of PPM to accurately simulate turbulent flows over a wide range of scales. More recently, Porter et al. (2002) discussed measures of intermittency in simulated *driven* transonic flows at Mach numbers of the order unity on grids up to 512^3 points. Porter et al. (1999) review the results of these numerical studies focusing on the origin and evolution of turbulent structures in physical space as well as on scaling laws for two-point structure functions. One of the important results of this fundamental work is the demonstration of compatibility of a Kolmogorov-type (Kolmogorov 1941, K41) spectrum with a *mild* gas compressibility at transonic Mach numbers.

Since most of the computations discussed above assume a perfect gas equation of state with the ratio of specific heats $\gamma = 7/5$ or $5/3$ and Mach numbers generally below 2, the question remains whether this result will still hold for near isothermal conditions and *hypersonic* Mach numbers characteristic of dense parts of star forming molecular clouds where the gas compressibility is much higher. What kind of coherent structures should one expect to see within the inertial range of scales in highly supersonic isothermal turbulence? Do low-order statistics of turbulence follow the K41 predictions closely in this regime? How intermittent is the turbulence? The interpretation of astronomical data from new surveys of cold ISM and dust in the Milky Way by *Spitzer* and *Herschel* satellites requires more detailed knowledge of these basic properties of supersonic turbulence.

In this paper we report first results from our large-scale numerical simulations of driven supersonic isothermal turbulence at Mach 6 with PPM and grid resolutions up to 1024^3 points. We solve the Euler equations in a periodic box of linear size $L = 1$ with initially uniform density distribution $\rho \equiv 1$ and the sound speed $c \equiv 1$. We initialize the simulation on a grid of 512^3 points with the random velocity field \mathbf{u}_0 that contains only large-scale power within the range of wavenumbers $k/k_{min} \in [1, 2]$, where $k_{min} = 2\pi$, and corresponds to the rms Mach number $M = 6$.

The same velocity field is then used, with an appropriate normalization, as a steady random force (acceleration) to keep the total kinetic energy within the box on an approximately constant level during the simulation. The random force is isotropic in terms of the total specific kinetic energy per dimension, $\langle u_{0,x}^2 \rangle = \langle u_{0,y}^2 \rangle = \langle u_{0,z}^2 \rangle$, but its solenoidal ($\nabla \cdot \mathbf{u}_0^s \equiv 0$) and dilatational ($\nabla \times \mathbf{u}_0^c \equiv 0$) components are anisotropic since one of the three directions is dominated by the large-scale compressional modes, while the other two are mostly solenoidal. The distribution of total specific kinetic energy $E \equiv \frac{1}{2} \int u^2 dV = E^s + E^c$ between the solenoidal E^s and dilatational E^c components is such that $\chi_0 \equiv E_0^s/E_0 \approx 0.6$. The driving field is helical, but the mean helicity is very low: $\langle h_0 \rangle \ll \sqrt{\langle h_0^2 \rangle}$, where the helicity h is defined as $h \equiv \mathbf{u} \cdot \nabla \times \mathbf{u}$. In compressible flows with an isothermal equation of state the mean helicity $\langle h \rangle$ is conserved, as in the

incompressible case, since the Ertel's potential vorticity is identically zero (Gaffet 1985).

We first ran the simulation on a grid of 512^3 points from the initial conditions up to five dynamical times to stir the gas within the box. The dynamical time is defined as $t_d \equiv L/(2M)$. Then we doubled the resolution and evolved the simulation for another $5t_d$ on a grid of 1024^3 points. We allow one dynamical time for relaxation at high resolution to reach a statistical steady state after re-gridding. The time-average statistics are computed using 170 snapshots evenly spaced in time over the final segment of $4t_d$. We use the full set of 170 snapshots to derive the density statistics, since the density field displays a very high degree of intermittency. This gives us a very large statistical sample, e.g. $\sim 2 \cdot 10^{11}$ measurements are available to determine the probability density function (PDF) of the gas density. The time-average power spectra discussed below are also based on the full data set. The velocity structure functions are derived from a sample of 20% of the snapshots covering the same period of $4t_d$. The corresponding two-point PDFs are built on $2 - 4 \times 10^9$ pairs per snapshot each, depending on the pair separation.

2. Results

Time evolution of global variables. The time variations of the rms Mach number and of the maximum gas density are shown in Fig. 1a, b. The kinetic energy oscillates between 18 and 22, roughly following the Mach number evolution. Notice the highly intermittent bursts of activity in the plot of $\rho_{max}(t)$. The time average enstrophy $\Omega \equiv \frac{1}{2} \int |\boldsymbol{\omega}|^2 dV \approx 10^5$ and the Taylor scale $\lambda \equiv \sqrt{\frac{5E}{\Omega}} \approx 0.03 = 30\Delta$, where Δ is the linear grid spacing and $\boldsymbol{\omega} \equiv \nabla \times \mathbf{u}$ is the vorticity. The rms helicity grows by a factor of 7.7 in the initial phase of the simulation and then remains roughly constant at a level of 1.2×10^3 . The conservation of the mean helicity is satisfied reasonably well as $\langle h \rangle$ is contained within $\pm 2\%$ of its rms value during the whole simulation.

Density PDF. In isothermal turbulence the gas density does not correlate with the local Mach number. As a result, the density PDF follows a lognormal distribution (Vázquez-Semadeni 1994; Padoan et al. 1997; Passot & Vázquez-Semadeni 1998; Nordlund & Padoan 1999). Fig. 1c shows our results for the time-average density PDF and its best-fit lognormal representation. The density distribution is very broad due to the very high degree of compressibility in isothermal supersonic conditions. The density contrast $\sim 10^6$ is orders of magnitude higher than in the transonic case at $\gamma = 1.4$ studied by Porter et al. (2002). Notice the excellent quality of the fit over more than eight decades in probability and a very low noise level in the data. If we express the standard deviation σ as a function of Mach number as $\sigma^2 = \ln(1 + b^2 M^2)$, we get the best-fit value of $b \approx 0.26$ that is smaller than $b \approx 0.5$ determined in Padoan et al. (1997) for supersonic MHD turbulence. The powerful intermittent bursts in $\rho_{max}(t)$ correspond to large departures from the time-average PDF caused by head-on collisions of strong shocks. These events are usually followed by strong rarefactions that are seen as large oscillations in the low density wing of the PDF and also in the density

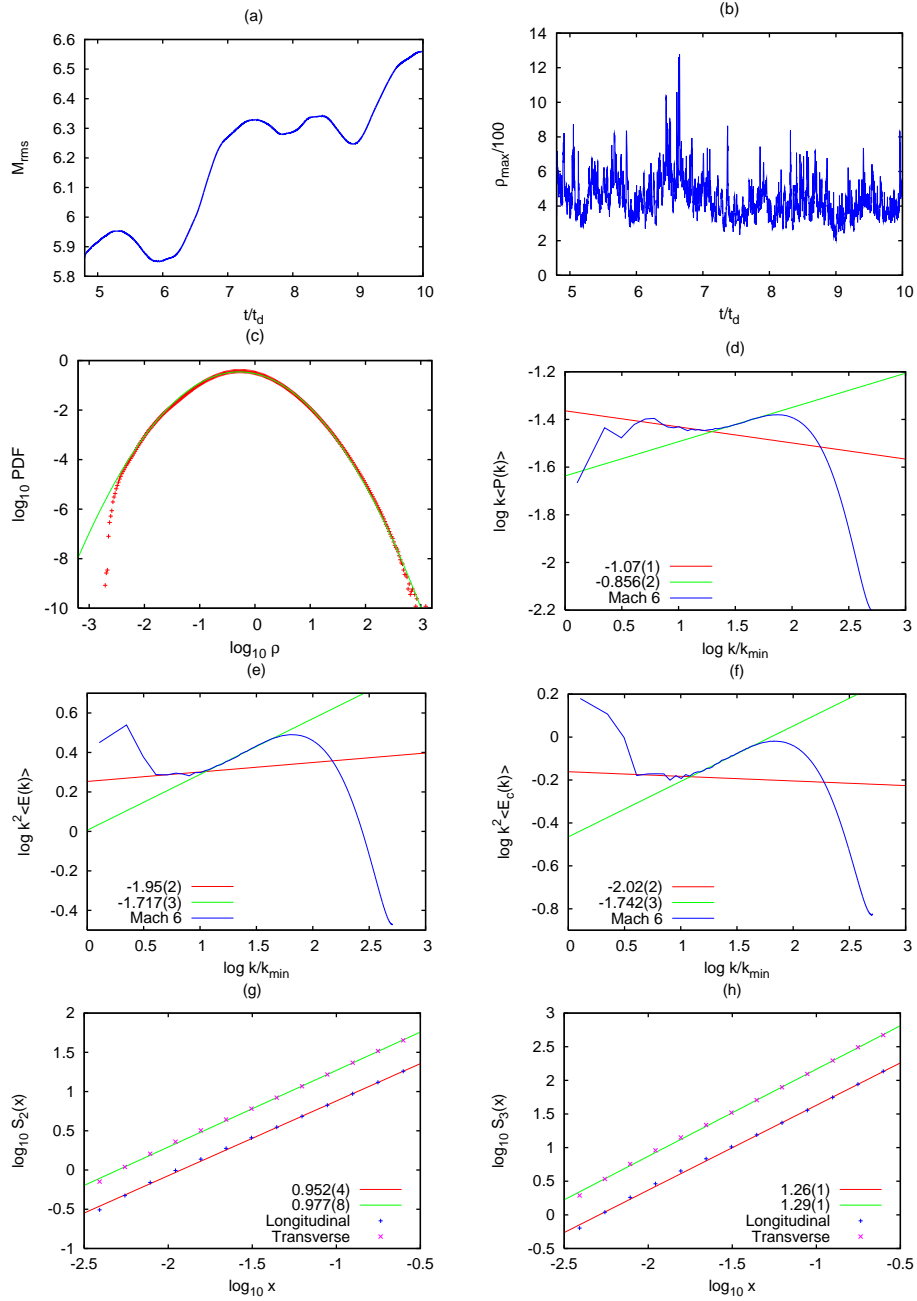


Figure 1. Results for the 1024³ simulation of driven Mach 6 turbulence with the ratio of specific heats $\gamma = 1.001$: (a) the time evolution of the rms Mach number; (b) the max density as a function of time; (c) the histogram for the gas density and the best-fit lognormal; (d) the density power spectrum compensated by k ; (e) the velocity power spectrum compensated by k^2 ; (f) the power spectrum of dilatational velocity compensated by k^2 ; (g) the 2nd order structure functions and the best-fit power laws for $\log_{10} x \in [-1.5, -0.5]$; (h) the 3rd order structure functions and the best-fit power laws for $\log_{10} x \in [-1.5, -0.5]$.

power spectrum. Intermittency is apparently present in supersonic turbulence. Its signature in turbulence statistics will be addressed elsewhere.

Inertial range scaling. The power spectrum of the gas density shows a short straight section with a slope of -1.07 ± 0.01 in the range of scales from 250Δ down to 40Δ followed by flattening due to a power pileup at higher wavenumbers, see Fig. 1d. A similar power-law section, although with a slope of -1.95 ± 0.02 , and an excess of power in the same near-dissipation range is also clearly seen in the velocity power spectrum, Fig. 1e. Apparently, the flattening of the spectra in the near-dissipation part of the inertial range is due to the so-called bottleneck effect related to a three-dimensional non-local mechanism of energy transfer between modes of differing length scales (Falkovich 1994). The same phenomenon has been observed both experimentally and in numerical simulations (e.g. Porter et al. 1994; Kaneda et al. 2003; Dobler et al. 2003; Haugen & Brandenburg 2004). At the resolution of 512^3 , the bottleneck effect at high wavenumbers and turbulence forcing at low k leave essentially no room for the uncontaminated inertial range in the k -space, even though the spectrum does show a nice power law. For the density power spectrum, we would get a slope of -0.90 ± 0.02 at 512^3 that is substantially shallower than -1.07 at 1024^3 . Thus, spectral index estimates based on low resolution simulations (e.g. Kim & Ryu 2005) may bear a rather large uncertainty. We also note that the time-averaging over many snapshots is essential to get the correct slope for the density power spectrum since it exhibits variations on a short (compared to t_d) time-scale. The spectrum tends to get shallower upon collisions of strong shocks, when the PDF's high density wing rises above its average lognormal representation.

The time-average velocity power spectra for the solenoidal and dilatational components show the inertial range power indices of -1.92 ± 0.02 and -2.02 ± 0.02 , respectively, see Fig. 1f for the k^2 -compensated dilatational spectrum. Both spectra display flattening due to bottleneck with indices of -1.70 and -1.74 in the near-dissipative range. The fraction of energy in dilatational modes quickly drops from about 50% at $k = k_{min}$ down to 30% at $k/k_{min} \approx 50$ and then returns back to a level of 45% at the Nyquist frequency.

Overall, the inertial range scaling of the velocity power spectrum in our highly compressible turbulence simulations tends to be closer to the Burgers scaling with a power index of -2 rather than to the K41 $-5/3$ -scaling suggested for the mildly compressible transonic simulations by Porter et al. (2002). To substantiate this result, we also computed the scaling properties of velocity structure functions $S_p(x) \equiv \langle |\mathbf{u}(\mathbf{r} + \mathbf{x}) - \mathbf{u}(\mathbf{r})|^p \rangle$ of the orders $p = 1, 2$, and 3 , where the averaging is taken for all positions \mathbf{r} and all orientations of \mathbf{x} within the computational domain. Both longitudinal ($\mathbf{u} \parallel \mathbf{x}$) and transverse ($\mathbf{u} \perp \mathbf{x}$) structure functions can be well approximated by power laws $S_p(x) \propto x^{\zeta_p}$, see Fig. 1g and h. The low-order structure functions are less susceptible to the bottleneck contamination and might be better suited for deriving the scaling exponents (Dobler et al. 2003).³ The best-fit 2nd order exponents measured

³Note, however, that the bottleneck corrections grow with the order p (Falkovich 1994) and influence the structure functions in a non-local fashion (Dobler et al. 2003).

for the range of scales between 32Δ and 256Δ , $\zeta_2^{\parallel} = 0.952 \pm 0.004$ and $\zeta_2^{\perp} = 0.977 \pm 0.008$ are substantially larger than the K41 predicted value of $2/3$ and agree well with our measured velocity power indices. The first order exponents $\zeta_1^{\parallel} = 0.533 \pm 0.002$ and $\zeta_1^{\perp} = 0.550 \pm 0.004$ are significantly larger than the K41 index of $1/3$. We find that the 3rd order scaling exponents $\zeta_3^{\parallel} = 1.26 \pm 0.01$ and $\zeta_3^{\perp} = 1.29 \pm 0.01$ are also noticeably off from unity predicted by K41 for the incompressible limit and also confirmed by Porter et al. (2002) for the transonic regime. Our measurements for the low order exponents roughly agree with the estimates $\zeta_1^{\perp} \approx 0.5$, $\zeta_2^{\perp} \approx 0.9$, and $\zeta_3^{\perp} \approx 1.3$ obtained by Boldyrev et al. (2002) for numerical simulations of isothermal Mach 10 MHD turbulence at a resolution of 500^3 points.

The large-scale driving force we used in these simulations is not perfectly isotropic due to the uneven distribution of power between the solenoidal and dilatational modes (perhaps, a typical situation for the interstellar conditions). We also use a *static* driving force that could potentially cause some anomalies on time-scales of many dynamical times. However, while strong anisotropies can significantly affect the scaling of high-order moments (Porter et al. 2002; Mininni et al. 2006), the departures from Kolmogorov-like scaling we observe in the lower order statistics appear to be too strong to be explained solely as a result of the specific properties of our driving. The sensitivity of our result to turbulence forcing remains to be verified with future high resolution simulations involving a variety of driving options.

3. Conclusions

Using high-resolution numerical simulations of nonmagnetic highly compressible turbulence at rms Mach number of 6, we have demonstrated that scaling exponents of low-order statistics deviate substantially from Kolmogorov laws for incompressible turbulence. A much higher than 1024^3 resolution is required to possibly trace a transition from a steeper supersonic inertial range scaling at lower k to a flatter Kolmogorov-like transonic scaling at higher wavenumbers.

Acknowledgments. This research was partially supported by a NASA ATP grant NNG056601G, by NSF grants AST-0507768 and AST-0607675, and by a NRAC allocation MCA098020S. We utilized computing resources provided by the San Diego Supercomputer Center.

References

- Boldyrev, S., Nordlund, Å., & Padoan, P. 2002, ApJ, 573, 678
 Colella, P. & Woodward, P. R. 1984, J. Comp. Phys., 54, 174
 Dobler, W., Haugen, N. E., Yousef, T. A., & Brandenburg, A. 2003, Phys. Rev. E, 68, 026304 1
 Falkovich, G. 1994, Phys. Fluids, 6, 1411
 Gaffet, B. 1985, J. Fluid Mech., 156, 141
 Haugen, N. E. & Brandenburg, A. 2004, Phys. Rev. E, 70, 026405 1
 Kaneda, Y., Ishihara, T., Yokokawa, M., Itakura, K., & Uno, A. 2003, Phys. Fluids, 15, L21
 Kaplan, S. A. & Pronik, V. I. 1953, Dokl. Akad. Nauk SSSR, 89, 643

- Kim, J. & Ryu, D. 2005, *ApJL*, 630, L45
- Kolmogorov, A. N. 1941, *Dokl. Akad. Nauk SSSR*, 30, 299
- Larson, R. B. 1981, *MNRAS*, 194, 809
- Mininni, P. D., Alexakis, A., & Pouquet, A. 2006, *ArXiv Physics e-prints*, 0602148
- Nordlund, Å. K. & Padoan, P. 1999, in *Interstellar Turbulence*, ed. J. Franco & A. Car-
raminana, 218
- Padoan, P., Nordlund, A., & Jones, B. J. T. 1997, *MNRAS*, 288, 145
- Passot, T., Pouquet, A., & Woodward, P. 1988, *A&A*, 197, 228
- Passot, T. & Vázquez-Semadeni, E. 1998, *Phys. Rev. E*, 58, 4501
- Porter, D., Pouquet, A., & Woodward, P. 2002, *Phys. Rev. E*, 66, 026301
- Porter, D. H., Pouquet, A., Sytine, I., & Woodward, P. 1999, *Physica A*, 263, 263
- Porter, D. H., Pouquet, A., & Woodward, P. R. 1992a, *Th. Comp. Fluid Dyn.*, 4, 13
- , 1992b, *Phys. Rev. Lett.*, 68, 3156
- , 1994, *Phys. Fluids*, 6, 2133
- Porter, D. H., Woodward, P. R., & Pouquet, A. 1998, *Phys. Fluids*, 10, 237
- Pouquet, A., Passot, T., & Leorat, J. 1991, in *IAU Symp. 147: Fragmentation of Molec-
ular Clouds and Star Formation*, ed. E. Falgarone, F. Boulanger, & G. Duvert,
101–118
- Sytine, I. V., Porter, D. H., Woodward, P. R., Hodson, S. W., & Winkler, K.-H. 2000,
J. Comp. Phys., 158, 225
- Vázquez-Semadeni, E. 1994, *ApJ*, 423, 681